

# A Real-Time Laser-Based Detection System for Measurement of Delineations of Moving Vehicles

Harry H. Cheng, Benjamin D. Shaw, Joe Palen, Jonathan E. Larson, Xudong Hu, and Kirk Van Katwyk

**Abstract**—In current practice, quantitative traffic data are most commonly acquired from inductive loops. In addition, video-image processing or time-of-flight laser systems can be used. These methods all have problems associated with them. We have developed a nonintrusive laser-based detection system for measurement of vehicle travel time. The basic detector unit consists of a fan angle laser and a photodetector array positioned above the plane of detection. This detection system is able to determine the length and width of moving objects in real time with high resolution, with the highest resolution measurements being associated with object lengths. This information is used to differentiate similar objects and can be used later for re-identification of individual objects or object groups, providing a real measure of travel time between detection sites.

**Index Terms**—Laser optical system, real-time vehicle detection.

## I. INTRODUCTION

TRAVEL TIME is the most important aspect of the Intelligent Transportation System (ITS). Travel time and travel time variance are good indicators of other direct constraints on ITS efficiency: cost, risk, and attentive workload. The importance of travel time is verified in Advanced Traveler Information Systems (ATIS) user surveys which indicate that what travelers most want from a transportation system is (almost always) reduced travel time and higher reliability. Every traveler must implicitly or explicitly make an assessment of these various travel time options before embarking on every trip; therefore this information is definitely of high value. Because trip travel time is the parameter the public most wants to minimize, this is the parameter that is most important for transportation service providers to measure and minimize.

Manuscript received July 1999; revised September 2000. Recommended by Technical Editor H. Peng. This work was supported with the funding from the California Department of Transportation through the PATH program at the University of California, Berkeley.

H. H. Cheng and B. D. Shaw are with the Integration Engineering Laboratory, Department of Mechanical and Aeronautical Engineering, University of California, Davis, CA 95616 USA (e-mail: hhcheng@ucdavis.edu).

J. Palen is with the Office of New Technology and Research, California Department of Transportation, MS 83, Sacramento, CA 94273 USA.

J. E. Larson was with the Integration Engineering Laboratory, Department of Mechanical and Aeronautical Engineering, University of California, Davis, CA 95616 USA. He is now with Applied Komatsu Technology American, Inc., M/S 9149, Santa Clara, CA 95054 USA.

X. Hu was with the Integration Engineering Laboratory, Department of Mechanical and Aeronautical Engineering, University of California, Davis, CA 95616 USA. He is now with the Center of Integration Engineering, Zhejiang Institute of Science and Technology, Hangzhou, Zhejiang, 310033 China.

K. Van Katwyk was with the Integration Engineering Laboratory, Department of Mechanical and Aeronautical Engineering, University of California, Davis, CA 95616 USA. He is now with Applied Materials, Inc., Santa Clara, CA 95054 USA.

Publisher Item Identifier S 1083-4435(01)04259-4.

Speed is commonly used as an indicator of the travel time across a link. In current practice, speed is measured at one or more points along a link and extrapolated across the rest of the link. This extrapolation method is used regardless of the mechanism of detection. Example detection methods are: loops—which determine speed from two elements spaced a known distance apart [1]; radar—which can directly determine speed from the carrier frequency shift (Doppler effect); or video image processing—which tracks vehicles across the pixel elements within the field of view [2], [3]. The extrapolation from a point to a line is not necessarily valid. At the onset of flow breakdown, the speed variations along the length of a link can be quite large. Also, the onset of flow breakdown is when routing decisions are most time-critical and accurate information has the highest value, so inaccurate extrapolations could have detrimental effects to the traveler.

An alternate method to determine the traverse travel time (e.g., the true link speed) is to use Vehicles As Probes (VAP). A VAP system determines travel time directly by identifying vehicles at the start of the link and re-identifying them at the end of the link, with the time difference being the true travel time. The problem with VAP systems is that they require large numbers of both vehicle tags and tag readers to be effective, and the cost justification of such a system may be unwarranted in light of other options. The key aspect to measuring the actual travel time is simply to identify some distinguishing characteristic on a vehicle at the beginning of a link and then to re-identify that same characteristic on the same vehicle at the end of the link. This is the basic idea of VAP, however the characteristic does not have to be entirely unique (as in a vehicle tag), and it does not necessitate the infrastructure set-up costs of VAP [4].

As an alternative to VAP's, if a characteristic can be found to separate a fleet into (say) 100 classifications, "the maximum probability fit" can be determined for the same sequence of classifications at the downstream detector as was identified at the upstream detector [5]. This is what is currently being done in Germany with the low-resolution imaging provided by (new high-speed) loops[4], and has been demonstrated in California. If a higher-resolution detector is used so that it is possible to get a few thousand classes, then it should be quite possible to perform 100% upstream-downstream Origin and Destination (O/D) identification using time gating and other relatively straightforward signal processing techniques (even if a significant percentage of the vehicles switch lanes). The mechanism of detection must allow highly resolved delineation between commonly available "commuter" vehicles, because commuter vehicles represent the majority of the vehicle stream during the period that traverse travel time information is most needed (e.g., the peak hours).

It is recognized that any mechanism to measure travel time, by definition, is only determining the “past state” of the transportation system. Collecting data on what happened in the past has no utility except if it is used to infer what may happen in the future. All decisions, by definition, are based on an inference of future consequences. When a traveler learns that speed on a route is 50 mph, the traveler generally infers that the speed will remain 50 MPH when she/he traverses it. This may or may not be a reasonable inference. Travelers want to know the “state” of the system (in the future) when they traverse it. In the simplest case, this is just a straight extrapolation of current “state.” More sophisticated travelers may develop their own internal conceptual model of the typical build up and progression of congestion along routes with which they are familiar. A major benefit of ITS will be to provide travelers with a much more valid and comprehensive “look ahead” model of the (short term) future state of the transportation system.

Validation of any traffic model requires (either implicitly or explicitly) traffic origin/destination (O/D) data. The lack of valid O/D data has been the major impediment in the calibration, validation, and usage of traffic models. This has led to the major motivation of this R&D effort: to develop a roadway detection system that can directly determine travel time and O/D data nonintrusively without violating the public’s privacy (as in license plate recognition systems).

With this roadway detection system, we have developed a nonintrusive laser-based detection system for objects moving across a planar surface (e.g., vehicles traveling along roadways). The basic detector unit consists of a fan angle laser, an image lens, a set of cylindrical optics and a photodetector array with the necessary circuitry positioned above the plane of detection. This system is configured such that it can unambiguously find the object boundaries in all lighting conditions independent of the time-of-flight of the laser. This paper presents basic ideas underlying the principles and design of the detection system. The detection system described here has been under development for some time, and some of our earlier work in this area can be found in a conference paper [6].

## II. RELATED WORK AND COMPARISON OF DIFFERENT DETECTION SCHEMES

Our detection system has a number of advantages over other systems currently in use. In current practice, vehicle features are most commonly measured using inductive loops or video image processing. An advantage of our system over loop detectors is the relative ease of installation and maintenance. Because loops are buried beneath the pavement, installation requires heavy equipment and traffic must be re-routed [7]. It is for this reason that loops are expensive to install and repair. Because our system is mounted above the road, once installed, it can be maintained without disrupting the flow of traffic. More importantly, loop detectors cannot be relied upon to produce accurate speed (and therefore length) measurements because the inductive properties of the loop and loop detectors vary [7]. Video can be used to directly measure the length of vehicles, however the use of real time video image processing is problematic due to its computationally intensive nature. Our system operates on a simple

“on/off” basis, requiring much less computation for vehicle detection, and consequently much less computational hardware. Because video is a passive system (gathering ambient light), video images are dependent on the lighting conditions. Vehicle length measurements taken from video, even on the same vehicle, may not produce consistent results depending on time of day and weather conditions. These limitations are related to variable lighting conditions and limited video camera dynamic ranges. For truly site and time independent vehicle length measurements, video would require an external source of illumination. Because our system is active, it produces its own signals to be sensed and it does not suffer from these limitations.

One system that bears some similarity to the system we have developed is the Automatic Vehicle Dimension Measurement System (AVDMS) developed by the University of Victoria, Canada, [8]. However, the AVDMS would not be suitable for our purposes. The AVDMS uses laser time-of-flight data to classify vehicles based on length, width, or height, and is based on the Schwartz Electro-Optics Autosense III sensor [9]–[12]. The Schwartz systems are entirely dependent on time-of-flight laser measurements with moving parts, similar to conventional lidar (laser radar). There are some significant functional differences between our system and Schwartz’s. For example, the fundamental mechanism of detection is that the Schwartz detector determines the range (or distance) from the detector to the objects being detected. Our detector functionally does not determine the range (or distance) from the detector to the objects being detected. The laser of the Schwartz’s detector reflects off the vehicle to determine the size, shape, and “presence” of the vehicle. In our detector, the laser reflects off the pavement. The lack of reflection from the pavement determines the size, shape, and “presence” of the vehicle. Therefore, our system will be more reliable because of its simplicity.

It is noted that other vehicle detection schemes exist or are presently under development. For example, video image processing has been used for some time as a vehicle detection system, and these types of systems are still undergoing research and development in an effort to obtain improvements. In future vehicle detection applications, the type of detector employed in the field will likely vary from location to location, depending on the strengths and weaknesses of each class of detector and the local needs at the application sites. Costs may also play a role, and it possible that video image processing systems may compete with a simpler system such as the one described in this paper.

In comparison with other conventional traffic detection techniques, our system will offer the following salient features.

- The system is mounted above the road and is relatively easy to install. Traffic need not be rerouted.
- The system is insensitive to ambient lighting conditions due to the active lighting source (the laser). It detects every passing object more than 46 cm (18 in) tall in all lighting conditions. No vehicles are missed, yielding nearly 100% accuracy.
- The laser and detector have no moving parts, giving the system high reliability. The primary raw data gathered by the sensor are computationally easy to process.

- Not only does the detector produce local vehicle speed, vehicle volume, and vehicle classifications, but it also allows highly deterministic re-identification of vehicles between sites, even under high flow conditions. Point-to-point travel time, incident detection, and O/D data can easily be determined with this detector.
- The system has very low power and communication bandwidth requirements, allowing the development of a solar-powered detector untethered from hard-wired infrastructure.

### III. METHODOLOGY

#### A. Functional Requirements of the Nonintrusive Detection System

If the primary purpose of a roadway detection system is redefined “to acquire unique or semi-unique information on vehicles and then reidentify them downstream,” then the functional requirements of this type of system can be determined. It must:

- be of high-enough resolution to delineate the vehicles;
- be reproducible enough to re-identify vehicles with site independence;
- be inexpensively deployable.

*Resolution:* For humans, resolving an image down so that it can be identified and reidentified is a relatively simple task. From a detection and information processing perspective, this isn’t nearly as simple. For example, a video image processing system would have to identify each of many moving “blobs”, scan each blob, segment it into parts (hood, door, tires. etc.), and integrate the segments into an (inferred) class, make or model, and store this information in a reproducible format which could be used for re-identification. This is computationally an extremely expensive task that would tax the capabilities of the most powerful computer available today. An optimized roadway based detector system should use the basic properties of the roadway to its advantage. Vehicles on a roadway lane almost always travel in one (longitudinal) direction. Therefore, there is no reason for the detector to scan in the longitudinal direction—it can simply have a number of quick but temporally offset samples at a fixed place in the road to acquire longitudinal delineation. Vehicles can also be laterally anywhere in a lane. Therefore, a detector needs to acquire information across almost the full width of a lane. Information acquired from any specific (roadway-detector) lateral orientation will be a function of the vehicle’s lateral position in the lane. Because vehicles tend to be more-or-less laterally symmetrical, it would be optimal for an overhead detector to integrate the information across the lateral direction and differentiate the information in the longitudinal direction to acquire the needed resolution for vehicle classification delineation.

*Reproducibility:* To be reproducible, the detector must be active, e.g., transmit its own energy that reflects off object(s) of interest the same way every time. The information acquired from passive detectors, which depend on light, heat or sound, varies with sun angle, trip distance, and speed—and therefore is not reproducible. The receiver of an active detector must be able to differentiate the active reflected energy from the natural background ambient energy in the same spectrum. This

may be accomplished in a number of ways: the detector transmitter may produce a very high power burst for a very small time period (often measured in nanoseconds) that oversaturates the background. The transmitter may transmit energy only over a very narrow spectrum and the receiver filters out all energy except that spectrum (such extreme narrow band filters can be expensive), or the transmitter may modulate energy at a high frequency and the ac output of the receiver filtered to remove components below that frequency. In practice, all three methods may be used in the most economical combination. Length can be directly measured through array processing systems (e.g., video), but this is generally noisy and inaccurate. It can also be determined from the vehicle’s instantaneous speed and residence time in the detection zone. Instantaneous speed can be directly acquired from the Doppler phase shifting of the energy transmitted from the detector and reflected off the vehicle, but this requires a relatively acute angle, which means the vehicle must be away from the detector where it would be difficult to acquire the needed delineating information with high resolution. Therefore, the instantaneous speed is most optimally acquired by precisely timing when the vehicle passes two adjacent detection zones a known distance apart. The tighter the timing and longitudinal resolution, the more precisely speed (and therefore length) can be determined. To be reproducible, an ideal detector would produce the same information independent of the view angle. However, the effective energy backscattered from an active detector is always contingent on the vehicle’s perceived cross section which changes with the view angle from the detector. The only parameters that can be reproducibly derived from any line-of-sight view angle orthogonal to the vehicle’s velocity vector are its (longitudinal) length and its color.

*Deployability:* Intrusive detectors that are embedded in the pavement are quite costly to install and maintain because the traffic must be moved out of the way to gain access. For any nonintrusive detector to work, it must have line-of-sight to the vehicles. This requires that it be mounted high enough to obtain an unoccluded view of all lanes. Because overhead structures are not always available at the most needed places for detection, a detector that can be side mounted would be much more deployable. Detection systems that require high-precision thermally-stable electronics, such as time-of-flight or Doppler phase shifting systems can be costly, complex, difficult to calibrate, and difficult to maintain. Systems based on a low number of simple, cheap, commonly available electronic components are desirable. Systems that have no mechanical moving parts generally require less maintenance. Computational complexity tends to increase with the number of detection elements and amount of noise per element. Video image processing systems analyze millions of relatively noisy pixels per second, and therefore tend to be computationally (and financially) expensive. Systems where the computational overhead can be handled by simple low cost CPU’s are desirable. The fiscal and administrative costs of running hard-wired cable to a detection site are often the single most significant limiting factor for deployment. Running cable may require traffic control, laying down K-rail, trenching, letting a minor contract, and budgeting many years in advance. A self-contained detection system that could be powered by photovoltaics and communicate through (non-FCC constrained) RF

would greatly enhance deployability. This self-powered self-communicating capability has been what has made call-boxes so popular.

### B. Vehicle Delineating Parameters

Of all the existing means of detection, loops, magnetometers, piezos, and tubes are intrusive. Acoustic is low resolution and subject to nonlinearity with thermal effects. Passive IR is low resolution and subject to nonlinearity with changes in ambient temperature. Doppler Radar lacks resolution and only works well at acute angles. Pulsed microwave backscatter produces a nonreproducible reflectance as a function of beam angle. Scanning laser time-of-flight systems are costly and have moving parts. What are we left with? Something that currently doesn't exist—a simple laser backscatter system combined with a robust “maximum probability fit” classification-sequencing algorithm. Lasers produce a tightly focused coherent beam of EM radiation at various frequencies. Spectral filters and/or modulation techniques can be used to discriminate the backscattered beam from the ambient background. The existing roadway laser based detection systems use the time-of-flight of a pulsed laser beam to determine the distance between the object and detector, but these systems require high precision electronics, which are quite expensive. All that is really needed for detection is to determine “if the laser is backscattering off the pavement” or “if it is reflecting off something else”. It can be assumed that “something else” is a vehicle. Using the laser, the following delineating parameters of a vehicle could be detected nonintrusively.

**Reflectance Signature:** This has the potential to be a highly delineating vehicle parameter. However, analogous to video image processing systems (VIPS), the high information density of a reflectance signature would be difficult to process into a reproducible parameter. Although laser reflectance signal processing would (most probably) be easier than that required for VIPS due to the controlled spectrum and consistent source-vehicle-detector geometries, one might expect very high reflectance outlines when parts of the vehicle body are exactly orthogonal to the transmitting laser vector. These might oversaturate the photo-diode detector. Therefore, this system would probably require multiple parallel lateral optical paths to reduce the effects of these outlines on the signature, with each path requiring a wide dynamic range high speed A/D converter. An advantage of this method is that the laser and return detector could be in the same optical path so that site specific focusing would not be necessary and fabrication would be relatively easy. A major disadvantage would be the high bandwidth signal processing and/or communication needed.

**Length:** This cannot (easily) be measured directly, but is calculated from the speed and residence time under the detector, both of which are ascertained simply from vehicle “presence”. “Presence” can be measured with divergent optical paths as shown in Fig. 1, allowing use of high-speed inexpensive digital samplers. From Fig. 1 we can determine the laser-receiver separation distance as a function of height as follows:

$$Y = \frac{X(H - H_c)}{H_c}. \quad (1)$$

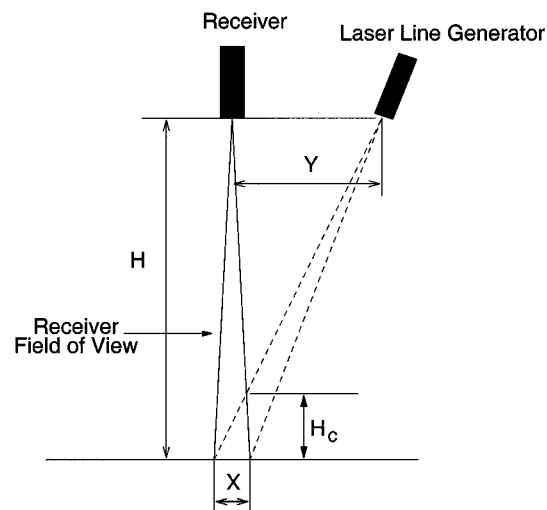


Fig. 1. Minimum object height.

In (1),  $H_c$  is the critical height, below which objects will not be sensed. Divergent optical paths will require some focusing, making fabrication and calibration slightly more difficult. Inherently, all other (spatially oriented) vehicle delineating parameters will have to be normalized by vehicle length to assure a consistent record format. It is not a question of “if” length should be measured; it is a question of “how accurate”. Length alone would appear to be a highly delineating parameter for passenger vehicles if measured with sufficient precision. The signal processing and communication requirements for length are smaller than for any other parameter.

**Overhead Profile:** An inherent problem with the measurement of vehicle length is that many, if not most, passenger vehicles have some curvature to their bumpers. Only the maximum vehicle length (usually along the lateral center-line of the vehicle) is reproducible. Because the vehicle may be anywhere within or between lanes, measurements need to be made across the full lane width to assure capture of the vehicle lateral center-line and, therefore, the maximum vehicle length. This will also provide the shape of the bumpers and vehicle width, which are additional delineating parameters.

It is also useful to discuss the relative merits of measurements of vehicle widths and lengths. The primary objective of the detector is to generate a unique feature vector that can re-correlated downstream at minimum computational expense (by rejecting each and every possible false match). Hence, a high-resolution scalar number is best (as opposed to an inductive signature waveform or video image, which must then be deterministically reduced to scalar numeric feature vectors for re-correlation). As a result, the best re-correlation feature vector is one that: (1) is measured with high resolution; (2) is measured with high accuracy that is site independent; and (3) measures a parameter with wide vehicle-to-vehicle variance. The length of a passenger vehicle typically varies from 12 to 20 ft, with trucks extending out to more than 90 ft. In contrast, the width of a passenger vehicle typically varies from 5 to 6.5 ft. Freeway lanes are 12 ft wide, and can be reduced down to 10 ft for construction projects, so even large trucks must fit in under this width. Hence, there is much greater variance in length than width.

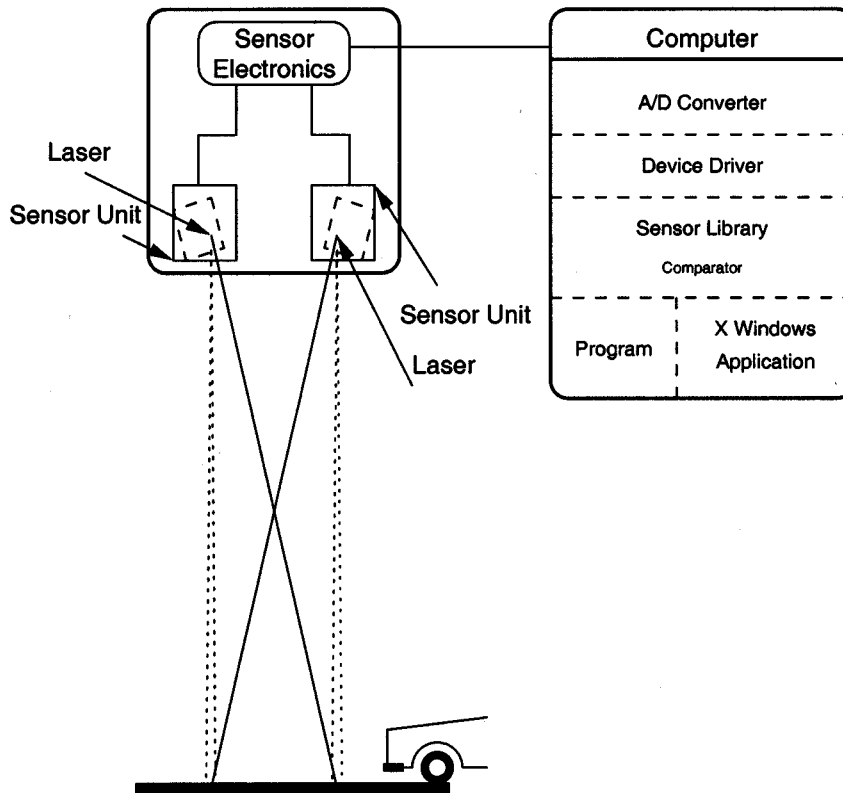


Fig. 2. System overview.

Width is also much harder to measure than length. Accurate measurement of any spatial parameter (height, width, or length) must be made orthogonal to the plane being measured. To accurately measure vehicle width from above, detection elements would be needed exactly above both sides of the vehicle. Because vehicle locations will vary across a lane, a continuous array of detection elements would be needed across all lanes. This procedure would be costly and logistically difficult.

To accurately measure length, a detector only needs to measure front and rear edge boundaries from the top down—small lateral offsets between the detector and vehicle make no difference. The vehicle moves itself in the “length” plane, aligning itself up with the orthogonal edge boundary laser detector. As a result, discrete concentrated detector elements can be used (a single detector for one, two, or three lanes), rather than having to have a continuous line of detector elements, as would be required for width. This capability to use discrete concentrated detector elements orthogonal to the velocity of the vehicles may eventually allow the use of the detector operating in a horizontal fashion, e.g., from a light pole. This configuration, which could not measure vehicle width, would work best for a small number of lanes. Horizontal operation mounts would also be cheaper and easier to install than overhead mounts. Hence, length is easier and cheaper to measure accurately than width, and it also provides greater vehicle-to-vehicle delineation.

*Color:* It is expected that the reflectance ratios of two different frequency lasers in the IR spectrum will be a function of the vehicle surface and therefore provide a consistent metric independent of orientation. This does require analog sampling,

but at a relatively low rate. If multiple samples are taken, the differential reflectance ratios for the nonpainted items (bumpers, windshield, etc.) can be easily rejected by making a histogram of the ratio values. The mode of this histogram should represent the largest surface area of the vehicle (which is painted). This represents relatively simple signal processing.

### C. System Overview

In our system, vehicle length is used as the primary identifying feature and is measured using two laser-based vehicle detectors. The system operates in the following manner, as illustrated in Fig. 2. The basic detector unit consists of a laser and a spatially offset photodetector positioned above the plane of detection. The laser is a pulsed infrared diode laser that utilizes line-generating optics that project to a flat planar surface where objects are to be detected. The detector consists of imaging optics and a linear photodiode array. The offset photodiode array receives the laser light that is reflected back from the region of detection. The signal from the photodiode is amplified and sent to a computer for processing. Vehicle presence is detected based on the absence of reflected laser light. Two of these units are integrated and placed a known distance apart, allowing the velocity of the object and its residence time under each detector to be measured, and giving the object’s length and top-down outline profile.

## IV. SYSTEM COMPONENTS

Fig. 3 shows the positioning of the system hardware. The detector is mounted at a distance of about 6.4 m (21 ft) (the height

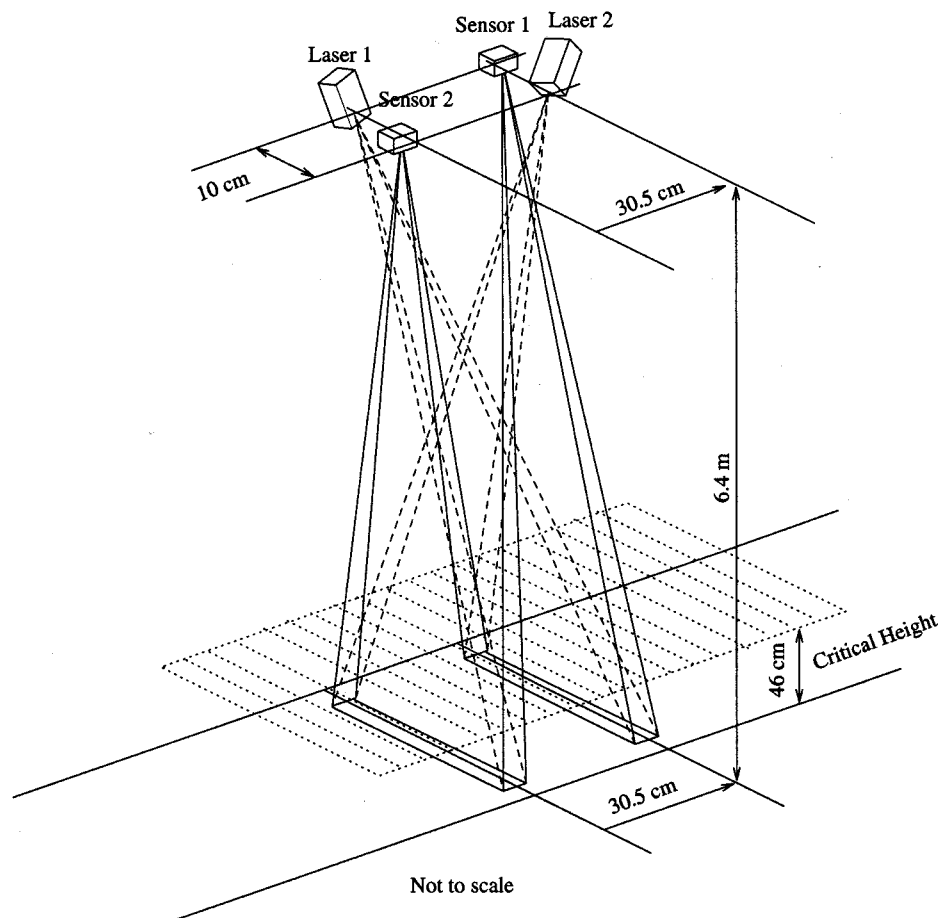


Fig. 3. System hardware configuration.

of a typical highway overpass) above the highway. The distance between each component of a laser/sensor pair is 30.5 cm (1.00 ft). The offset between the two sensor pairs is 10 cm (4 in). The sensors are mounted in a fixed vertical position, pointing downward, and are focused on the ground, forming two detection zones. The lasers are pointed toward the detection zones and are mounted at an adjustable angle, allowing the system to be mounted at different heights. The detection zones stretch across the width of the lane and are each about 13 mm (0.5 in) wide in the direction of traffic flow. In this configuration the minimum detectable object height, also called the critical height, is about 46 cm (18 in). This is lower than the bumper height of most common vehicles. For objects below this height, the laser line will still be visible by the sensor. This can result in the object remaining undetected or can cause a signal spike due to reflections, depending on the surface properties and geometry or the object. In either case, for vehicle bumper heights below the critical height, the speed and length measurements will be incorrect due to the fact that one or more of the vehicle edges will be incorrectly found.

When a vehicle moves into a detection zone, it blocks the laser from being received by the sensor, as shown in Fig. 4. When the first beam is blocked the time is recorded. When the second beam is blocked, a second time is recorded. These times give the speed of the front of the car. In a similar manner, when each of the beams is no longer blocked, as shown in Fig. 5,

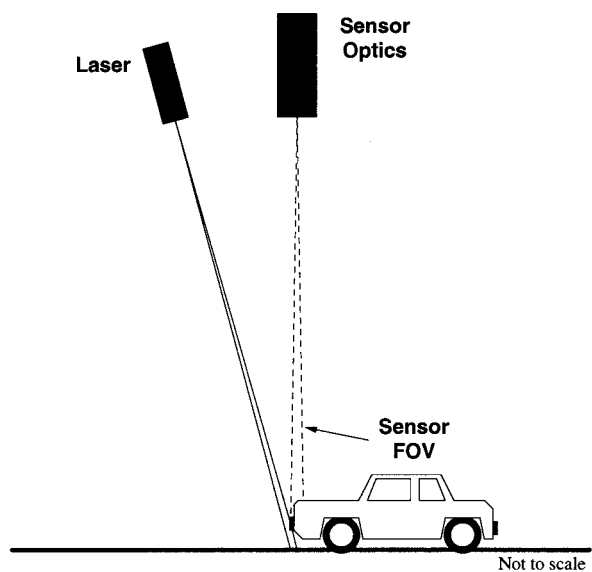


Fig. 4. Vehicle entering a detection zone.

the times are recorded and the speed of the rear of the vehicle can be calculated. The time that each detector is blocked is also recorded and is used to calculate the vehicle length, assuming constant vehicle acceleration. A more detailed description of the speed and length measurement algorithms is presented in

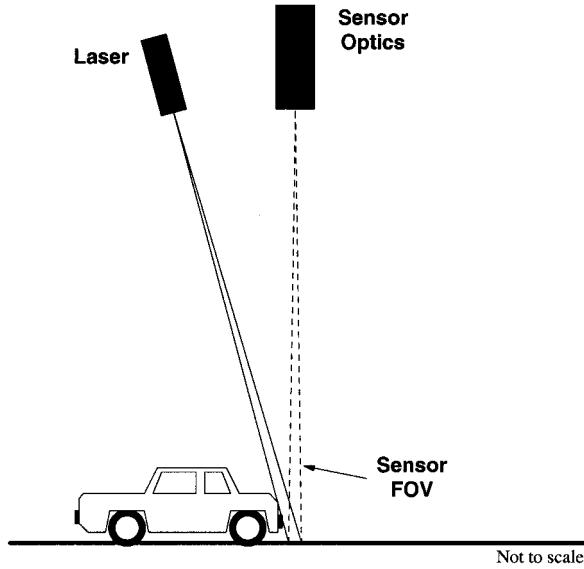


Fig. 5. Vehicle exiting a detection zone.

the software section. The assumption of constant acceleration is valid for free-flow traffic conditions, where there is negligible acceleration, and for conditions where the vehicle is accelerating or decelerating uniformly during the time it is in the detection zone. These cover the majority of situations, but there are a few situations, such as stop-and-go traffic, where this basic detection method will not necessarily yield highly accurate vehicle lengths.

#### A. Sensor Optics

The sensor optics consists of three main components: an imaging lens system, a telescopic lens system, and a bandpass filter.

The imaging lens system focuses the reflected laser light onto the active area of the sensor array. The imaging lens was selected based on the criteria that it should have an adjustable focal length within a range around the desired focal length, that it should have a field-of-view large enough to capture the width of an entire lane and that it should be compact for easy integration into the outdoor system.

Based on the assumptions that the lane width ( $h_o$ ) is around 3.05 m (10.0 ft) and that the unit will be mounted about 6.40 m (21.0 ft) above the roadway ( $s_o$ ) and given that the sensor is 7.5 mm (0.295 in) long ( $h_i$ ), an image distance ( $s_i$ ) was calculated for the sensor using (2), where it was determined that  $s_i = 15.8$  mm (0.620 in).

$$s_i = s_o \frac{h_i}{h_o}. \quad (2)$$

The desired focal length ( $f$ ) of the lens was then calculated using (3).

$$f = \frac{1}{\frac{1}{s_i} + \frac{1}{s_o}}. \quad (3)$$

The focal length was calculated to be 15.7 mm (0.616 in). As a practical matter, the sensor array is placed at the focal point

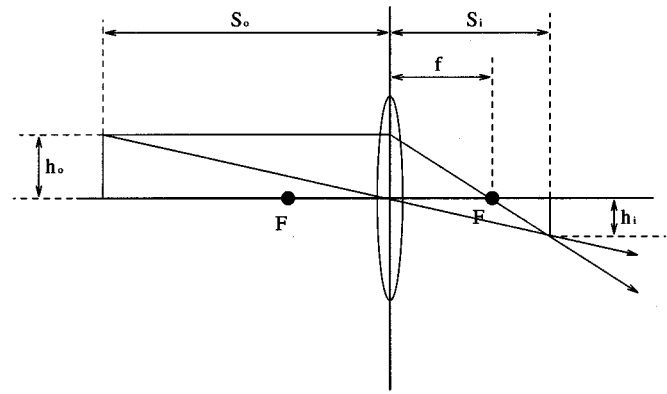


Fig. 6. Lens parameters.

of the imaging lens system. Because  $s_o$  is large in comparison with  $s_i$ ,  $f$  is nearly equal to  $s_i$ .

The lens we selected, a Tamron 23VM816, has an adjustable focal length of between 0.315 in (8 mm) and 0.630 in (16 mm) and was selected because of this feature. The Tamron lens is also suitably compact and has a field of view that is large enough to capture the entire lane width. Any lens system that has the correct focal length and an acceptable field-of-view could be used.

The telescopic lens system is mounted in front of the imaging lens system. It is designed to restrict the field-of-view of the imaging lens along the width of the laser line, but not alter the field-of-view along the length of the line. Because the laser line is much longer than it is wide, use of the imaging lens alone would result in a much wider strip of pavement being visible to the sensor than is desired. The telescopic lens system is used to match the dimensions of the laser line image with those of the sensor array.

The telescopic lens system consists of one positive plano-cylindrical lens and one negative plano-cylindrical lens. The prototype uses a 150-mm focal length cylindrical lens and a 19-mm focal length cylindrical lens both manufactured by Melles Griot Inc. These lenses are positioned to form a Galilean telescope. When positioned correctly the cylindrical lenses will not affect the proper operation of the imaging lens. The ratio of the focal length of these lenses is approximately equal to the ratio of the uncorrected field-of-view of the width of the sensor to the desired field-of view. The desired field-of-view,  $X$ , is determined based on (4), where  $Y$  is the separation of the sensor and laser,  $H$  is the height of the system above the road, and  $H_c$  is the desired minimum detectable object height, as shown in Fig. 1. To insure reliable vehicle detection, it is important that  $H_c$  be below the bumper height of most common vehicles.

$$X = \frac{H_c Y}{H - H_c}. \quad (4)$$

The uncorrected field of view, about 13 cm (5 in), results in a critical height of about 1.8 m (6.0 ft). To ensure vehicle detection it is necessary to have a critical height somewhere below the bumper height of the vehicles. A height of around 46 cm (18 in) was thought to be acceptable. To achieve this it is necessary to restrict the field of view  $X$  to about 2.3 cm (0.92 in). This

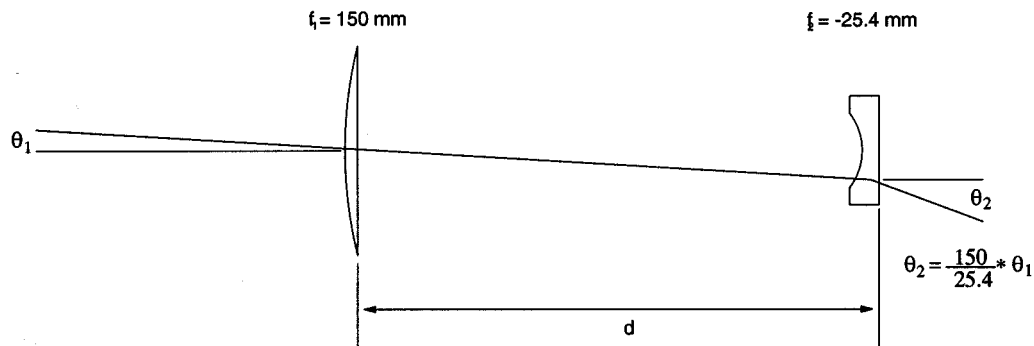


Fig. 7. Telescopic lens system.

is a factor of reduction of about 5. In our case, where  $f_1 = 150$  mm and  $f_2 = -19$  mm, the factor of reduction is equal to about  $-7.9$  (the negative sign indicates an inverted image), giving us a field of view of about 16 mm (0.63 in). The factor of reduction is commonly referred to as the angular magnification of the system. As shown in Fig. 7, a ray of light entering the system from the left at an angle  $\theta_1$  exits the system at the right at an angle  $\theta_2$  equal to  $\theta_1 \cdot f_1/f_2$ . Because of this, objects to the left appear to be larger than they actually are. This is how the field of view is reduced. A sensor on the right of the telescopic system will have its field of view reduced by a factor equal to the angular magnification of the system. The telescopic system does not alter the position or focus of the image. Objects that are properly focused by the imaging lens remain in focus when the telescopic system is added.

From Fig. 1 it is apparent the while the angular field of view of a receiver is constant (i.e., it is fixed by the optics), the distance  $X$  along the roadway that is viewed by the receiver depends on the height  $H$ , i.e.,  $X = YH_c/(H - H_c)$ . Vibrations of the support structure will cause variations in  $H$  and hence, variations in  $X$ . For the representative values  $Y = 0.305$  m,  $H = 6.4$  m, and  $H_c = 0.46$  m it is found that  $X = 0.0236$  m (2.36 cm). If the support structure vibrates such that variations in  $H$  of  $\pm 0.05$  m (5 cm) occur (these are large vibrations), the  $X$  values will cover the range 0.0116–0.0120 m (1.16–1.20 cm). The resulting percentage changes in  $X$  are very small (about  $\pm 0.8\%$ ), even with these large vibrations, and as a result the effects of support vibration on the field of view should not be significant.

A bandpass filter that is matched with the wavelength of the laser is used to reduce the level of ambient light received by the sensor. The filter is mounted between the telescopic and imaging lens systems. The filter used in the prototype is manufactured by Omega Optical Inc. (model 904DF15). This filter has a full-width half-maximum bandwidth of 15 nm centered at 904 nm. This filter is mounted on a ring that is threaded onto the front of the imaging lens.

### B. System Electronics

A block diagram of the prototype hardware construct is shown in Fig. 8. The hardware can be divided into five main parts: the power supply, the clock pulse generator, the laser components, the sensor circuit, and the A/D converter and computer.

**Power Supply Section:** The power supply section delivers power to both the laser components and the sensor circuit. There are several different voltages needed by the system. A triple output power supply provides +12 V,  $-12$  V, and +5 V. The +5-V output is used to power to the clock generator. The +12-V output supplies power to the laser system and the dc/dc converter required for the sensor array. A high voltage dc/dc converter changes 12 V dc to 250 V~350 V dc and is used to bias the sensor array to  $-290$  V. The sensor circuit (except for the pre-amplifier) uses both the +12 V and  $-12$ -V outputs. For our triple-output dc power supply, the maximum output ripple is 5-mV peak-to-peak value. This is a little large for a weak-signal amplifier power supply. In addition, the pulse laser consumes a large amount of power when the laser is on. According to the data sheet of the laser system, the momentary current will reach up to 20 A. This large current drain pulse will cause additional noise in the output voltage of power supply. Using a separate power supply for the pre-amplifier avoids this and increases the signal quality. In the system, a linear encapsulated power module, which produces  $\pm 5$  V, is used to power the pre-amplifier. The maximum output ripple of this power supply is 1-mV peak-to-peak value.

**Clock Pulse Generator Section:** The clock generator provides a clock signal that is used to trigger the laser and to synchronize it with the sampling of the photodiode sensor. In our system, an LM555 is used as the oscillator, as shown in Fig. 9. A 15-ns pulsewidth 2.2-kHz clock signal was chosen to operate the laser system. The frequency and width of the pulse can be chosen by adjusting the values of resistors  $R_a$  and  $R_b$ . Increasing the value of  $R_a$  will increase the pulse frequency and increasing the value of  $R_b$  will increase the pulsewidth. In the near future, we will increase the clock frequency to 10 kHz.

**Laser Components Section:** An off-the-shelf integrated diode laser system is used as the laser source. This system incorporates a DC/DC converter, power regulator, laser diode, and laser line generator into a single unit. The laser wavelength is  $905 \pm 10$  nm with a pulsewidth of 15 ns and a maximum pulse rate of 10 kHz. The laser's output power (peak) is about 20 W with an operating current (quiescent) 28 mA. The line-generating optics produce a beam with a full fan angle of 37 degrees.

**Sensor Circuit Section:** A 25-element avalanche photodiode (APD) array is used as the sensor in our detection system,



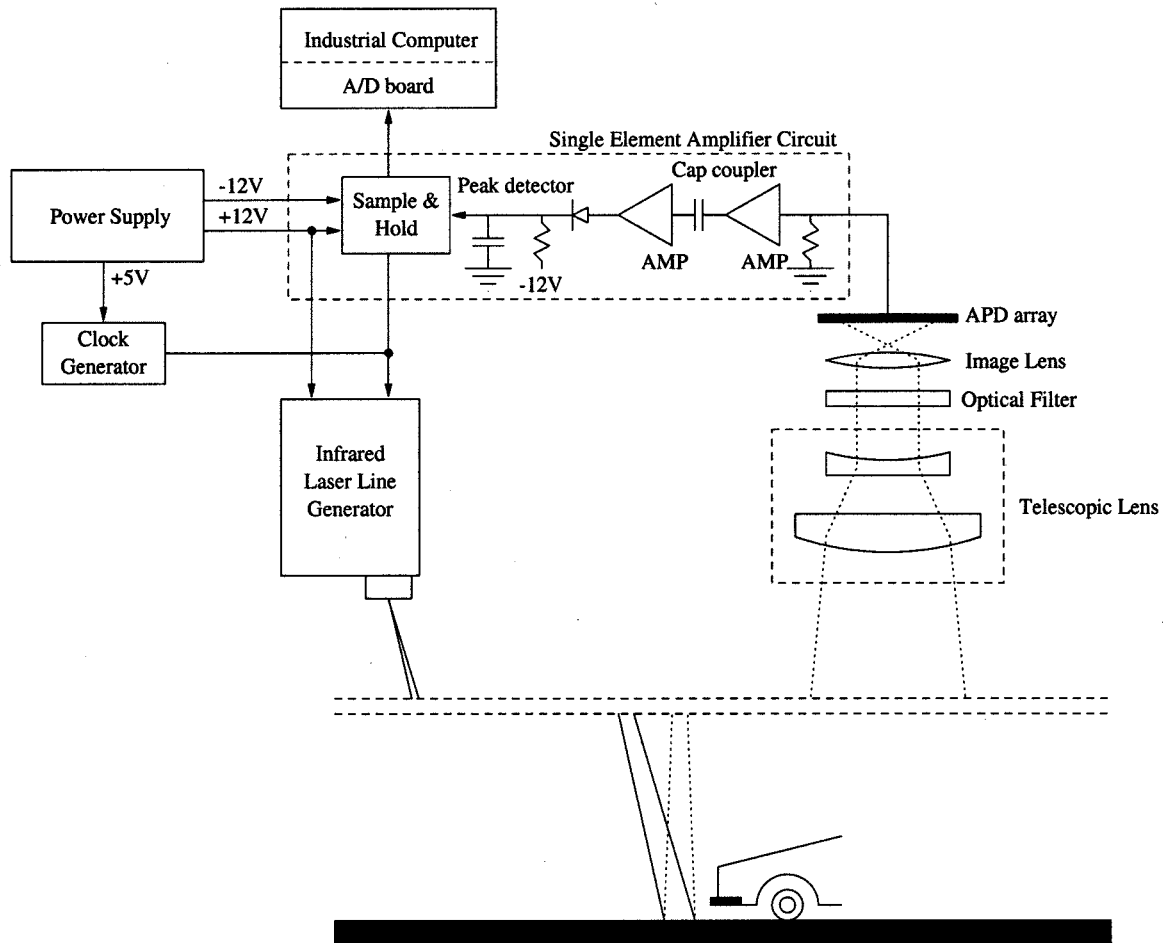


Fig. 8. Diagram of electronics hardware.

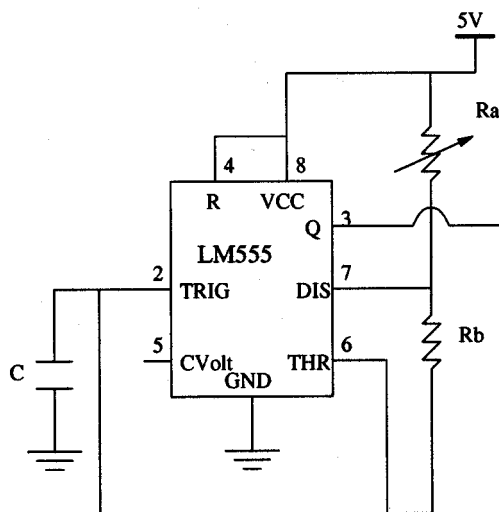


Fig. 9. Clock circuit.

though currently only four elements of each array are used. In the future we plan to use all elements of the array. The sensor converts the reflected laser light into a current signal. The sensor circuit is the main part of the electronic hardware in the detection system. This circuit conditions and amplifies

the signal produced by a single element of the sensor array so that it is suitable for sampling by the data acquisition board. Each element of the sensor that is used has its own circuit as described below.

The circuit can be divided into three stages: signal conditioning and amplification, peak detection, and sample/hold, as shown in Fig. 10. The current produced by a sensor element is converted to a voltage by U1. U1 is a low-noise, high-speed amplifier and is used in a noninverting configuration. C2 is a small value capacitor used for noise reduction. The signal is then passed through a resistor, R4, and a capacitor, C7, which filters out the DC or low frequency signals components from the previous stage. U2 is used as an inverting amplifier. The signal is amplified to a suitable value for the computer. Similar to the pre-amplifier stage, C9 is used to further reduce the noise. The amplified signal is a voltage pulse. The peak detector is needed to pick up the signal peak and deliver it to the sample & hold circuit. D2 and C14 consist of a peak detector. The output of the amplifier stage charges C14 through diode D2. The highest point of the output waveform of the amplifier is held by C14 while the diode D2 is back-biased. R7 and a -12 V power supply are used to reset the capacitor C14. The detected peak is then input to the sample-and-hold circuit. This circuit uses the same clock pulse that is used as a trigger by the laser to synchronize the sampling of the signal with the laser pulse. C3, C4,

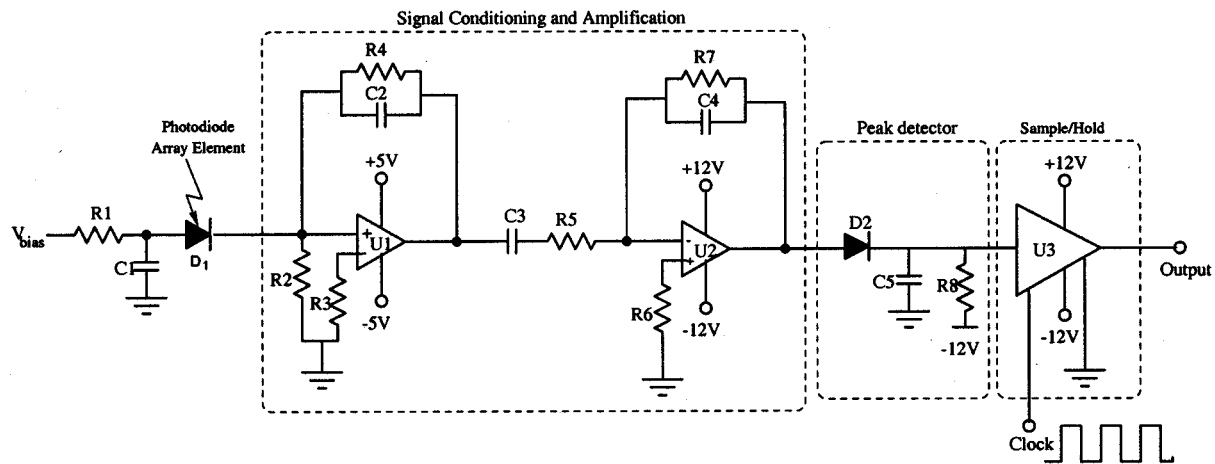


Fig. 10. Sensor circuit.

C5, C6 and C10, C11, C12, and C13 are de-coupling capacitors which filter noise from the power supply.

## V. SENSOR FIELD OF VIEW

During indoor resting, each of the 25 APD sensor elements was tested to verify the size of the field of view and the location of each element. In doing so, a reflective strip was moved in small increments across the entire length of the laser line, which was placed approximately 18 ft from the sensor, and the sensor signal level was recorded. The sensor produced a negative voltage in response to the laser, so reflections can be seen as large negative values. Fig. 11 shows the signals for three representative elements. As can be seen in this figure, the separation between adjacent points of maximum reflection (labeled a, b, and c in Fig. 11 along the length of the laser line is approximately 4 in at a distance of 18 ft, consistent with our calculations. Note that the signal level was recorded with a resolution of 0.1 V using an oscilloscope.

## VI. A/D CONVERTER AND COMPUTER SECTION

The output from the sample-and-hold is an analog signal that must be digitized for processing. A PC-based, 16-channel A/D board installed in an industrial computer is used for this purpose. The converted digital data is then sent to the computer through the data bus for further handling. The main computer used in the system is an industrial Pentium computer. Custom software is used for processing of the data.

### A. Software

The purpose of the laser detector software is to collect, process and display vehicle delineation data, all in real-time. The software is separated into layers by function, as shown in Fig. 12. Each layer performs a specific function and hides the implementation from other layers. The layers interact and pass data by using function calls. The detection system software runs under the LynxOS real-time operating system. LynxOS from Lynx Real-Time Systems, Inc., is a UNIX compatible, highly deterministic operating system for embedded applications [13]. The operating system was used for its hard

real-time, priority-based scheduler and implementation of kernel threads, POSIX threads and thread synchronization. The LynxOS scheduler always executes the highest priority kernel or user-level thread, performing fast context switches between threads. Interrupt service routines are implemented using high priority kernel threads, which allow the operating system to be responsive and predictable. LynxOS is conformant to a portable operating system interface standard, known as POSIX. POSIX is a source code interface standard that specifies a set of facilities for real-time programming [14]. The detection software uses POSIX threads and counting semaphores to prioritize and synchronize the various tasks involved in collecting, processing and displaying the vehicle delineation data.

The bottom most layer is the computer hardware that obtains the data from the detector and converts the data to digital form. The first layer of software is the device driver that communicates with the computer hardware in a low-level fashion. The interface to the data acquisition device driver occurs through standard function calls, such as `open()`, `close()`, `read()`, `write()` and `ioctl()`. The device driver hides the low-level interaction between the data acquisition hardware so the rest of the sensor software does not have to be burdened with low-level communication. The device driver uses a circular queue to buffer the data while it is continuously collecting data from the data acquisition board so no data is lost between requests for the data.

The sensor library layer requests detector data from the device driver and processes the data for applications and other software libraries. Both the vehicle delineation library and the applications in the top layer of the software use the sensor library. A TCP/IP server is used to send the vehicle data over a network, X Window System applications are used to display the detector and vehicle data in real-time and a user program is used to perform simple operations on the data.

*Sensor Library:* The sensor library is the largest portion of the software that obtains detector data from the data acquisition device driver and processes the data for other applications and software libraries. The sensor library requests data from the device driver in a specified block size. The library converts the data from digitized values to various forms. The library consists of various levels of functionality. The library is multi-tasking and

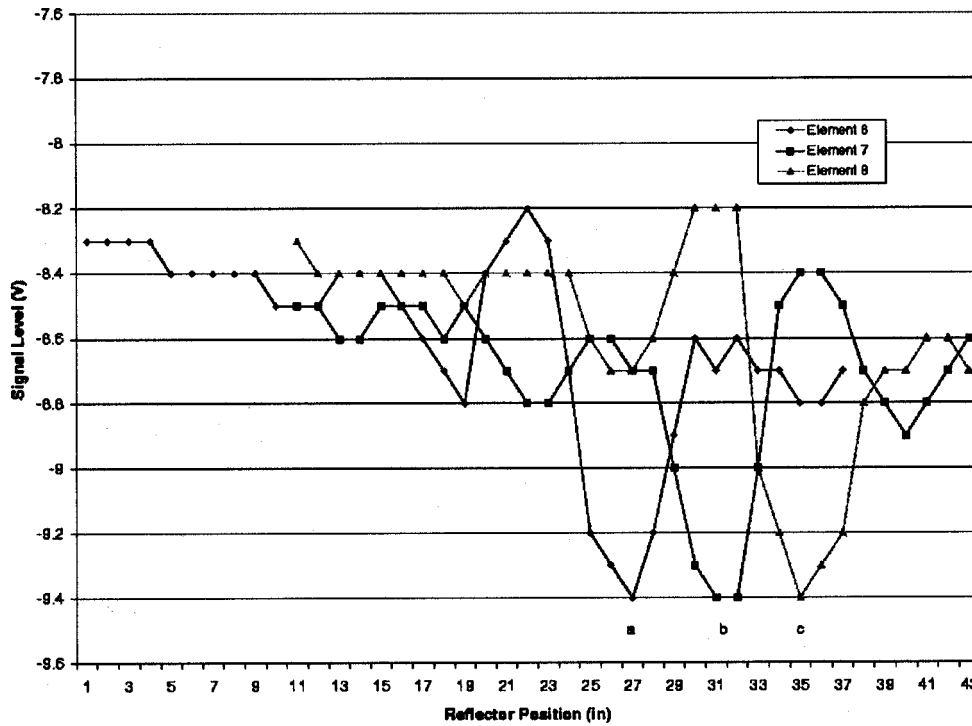


Fig. 11. Data showing laser signal separations between adjacent APD detector elements.

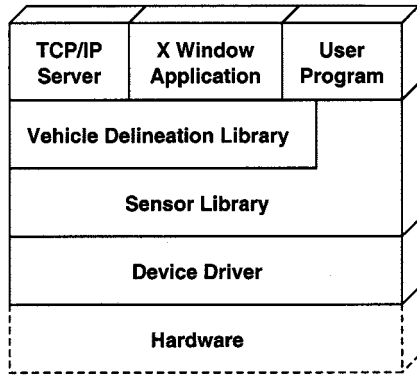


Fig. 12. Laser detector software layers.

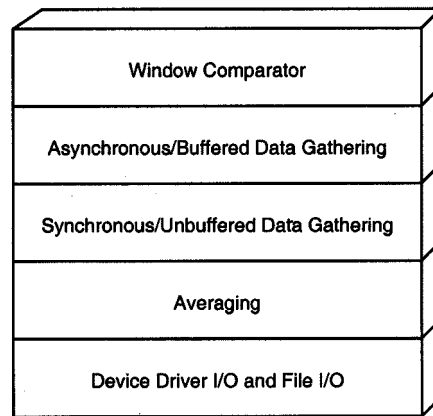


Fig. 13. The layers of the sensor library.

multi-threaded. It is multi-tasking because various tasks must occur simultaneously. Multi-tasking is implemented by using threads that run at separate scheduling priorities. A thread at a higher priority blocks other threads from running. Using priority-based threads increases the responsiveness of the software for real-time data acquisition.

Fig. 13 shows the separate modules of the sensor library. At the bottom is the device driver function calls and the file input and output function calls. The next layer is the averaging layer that computes the running average of the sensor signal. The Synchronous/Unbuffered Data Gathering layer is the layer that sets up and gathers the data from the device driver. This layer contains the highest priority thread that encompasses the averaging layer and device driver and file I/O layer. The layer is synchronous because the interaction between the high priority

thread and the application is synchronized. It is unbuffered because no buffer exists between the thread and the application requesting the data.

The next layer is the Asynchronous/Buffered Data Gathering layer. This layer sets up and uses a buffer that allows asynchronous requests of data while the high priority thread reads the data and stores them in the buffer. This scheme is desirable because the application does not directly affect the gathering of data. As a result, no data are lost.

The top most layer of the sensor library is the window comparator. The window comparator converts floating-point signal values to detection states, which indicate whether or not the laser is blocked. A blocked laser indicates the presence of a vehicle for that particular element of the photodiode array. The comparator is configurable during run time to be more responsive to changing signal conditions.

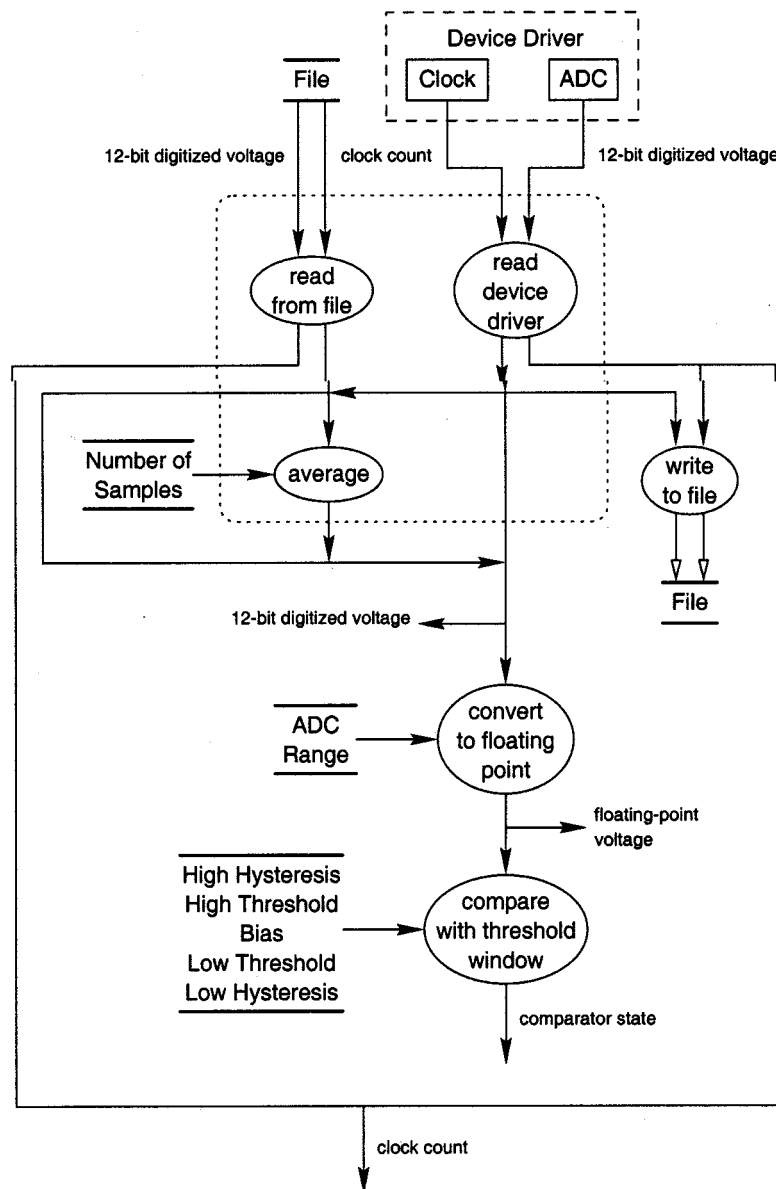


Fig. 14. Functional diagram of the sensor software library.

Fig. 14 shows the functional diagram of the sensor library, which shows the data flow between the separate functions and modules. The sensor library requests data from the device driver as though it was directly requesting data from the analog-to-digital converter (ADC) and the clock on the data acquisition hardware. Data from the ADC are in the form of 12-bit digitized voltage values. The clock count is a 32-bit number representing the time. Each block of data contains a clock count so each sample of data can be linked directly to an instant in time. The sensor library has the option to save the clock counts and digitized values to a file for later playback or use the values directly from the device driver. The averaging function of the sensor library converts a specified number of samples to a single average voltage. This is done to eliminate random noise read from the ADC. The reading of the device driver, the file reading and averaging are all performed within a thread that is scheduled at a high priority. The writing of data to a file is contained within a

low priority thread so the gathering of data is not interrupted. All other functions are within the same priority of the application program using the sensor library.

Next, the digitized values are converted to floating-point voltages by dividing the digitized value by the total voltage range of the ADC. Once the data has been converted, the voltages can be used directly and passed through a window comparator. The window comparator portion of the sensor library converts the voltage values to a comparator state. The comparator consists of a window bordered by a high threshold level and a low threshold level. The software compares the current voltage value with the high and low threshold values. When the value is between the two thresholds, the state of the comparator is false and when the value is above or below the threshold, the comparator state is true. Before the software compares the value to the threshold levels, it removes a bias voltage value. The bias voltage value is the level of the ADC when the laser is blocked.

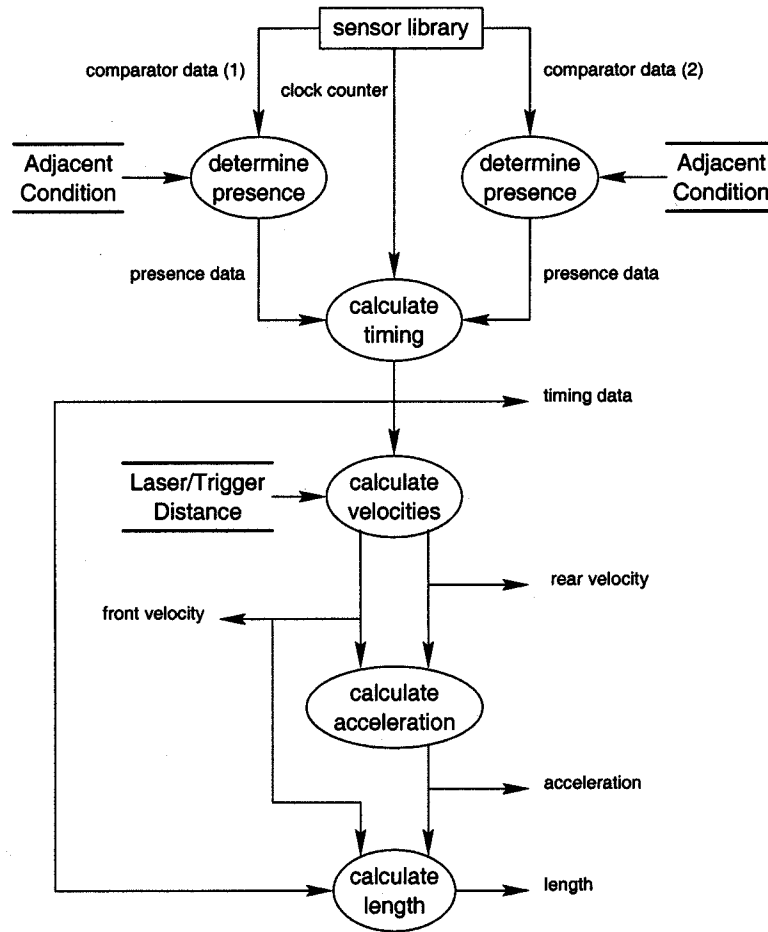


Fig. 15. The functional diagram of the vehicle delineation library.

In other words, the software comparator removes the ambient light from the voltage value to only compare the signal of the laser to the threshold levels.

One problem with window comparators is how they handle noise. Rapid transitions across the threshold levels cause the comparator state to change rapidly. To remedy this problem, feedback or hysteresis is used to eliminate rapid changes of state due to noisy signals. An electrical hardware device that implements this is known as a Schmitt trigger [15], which is implemented here via software. The trigger uses a small envelope to essentially widen the threshold level the signal would have to pass completely *through* for the comparator to change states. The size of the envelope for the high threshold level is specified by the high threshold level on the bottom and the high hysteresis level on top. The size of the envelope for the low threshold level is specified by low threshold level on the top and low hysteresis level on the bottom. The envelope size is adjusted according to the noise level of the signal to eliminate rapid changes in comparator states.

**Vehicle Delineation Library:** The purpose of the vehicle delineation library is to convert sensor library data to vehicle delineation data, such as vehicle timing information, front velocity, rear velocity, average acceleration and ultimately length. Fig. 15 shows the functional diagram of the vehicle delineation library,

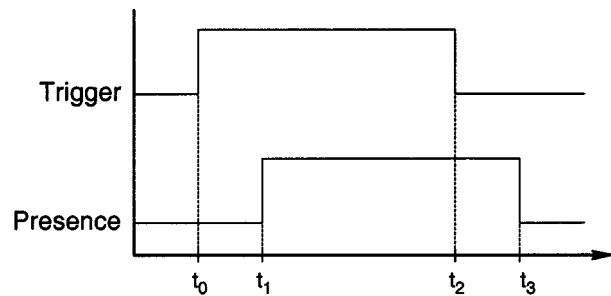


Fig. 16. The timing diagram when a vehicle passes under two sensors.

indicating the flow of data between the functional aspects of the library. The vehicle library obtains comparator data from the sensor library and determines if a vehicle is present based on the comparator states of the photodiode array. The library examines the comparator states of each element of the array. A vehicle is considered present when a specified number of adjacent comparator states are true. Essentially, the library converts a series of comparator states for the photodiode array to a single vehicle presence state.

Once the presence state is determined, the software calculates the timing of the front of the vehicle and the rear of the vehicle. If the presence state is false, no timing will be calculated. The

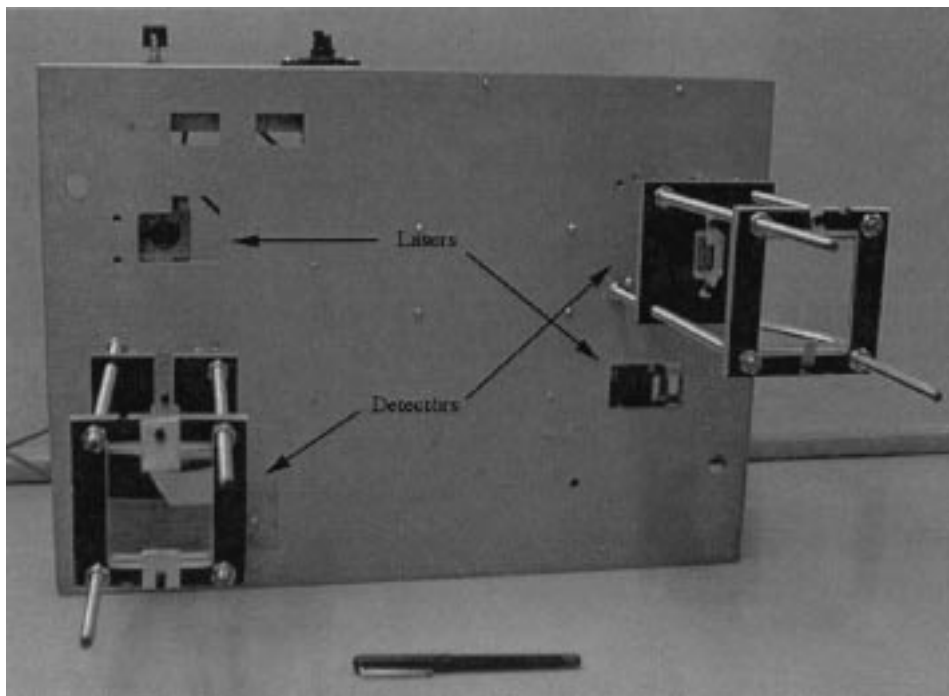


Fig. 17. Close-up of the front of the detection system.

vehicle passes under the first sensor and the software indicates that the vehicle is present for that particular sensor. Then the vehicle passes under the second sensor and the software indicates it is present for that sensor. The vehicle library calculates the time between the edges of the presence states of the two sensors using the clock count from the sensor library. A clock count is associated with each block of data so each instant of time of every sample of data can be calculated. Fig. 16 shows the timing of the two sensors. The front of the vehicle is indicated by times  $t_0$  and  $t_1$  and the rear of the vehicle is indicated by  $t_2$  and  $t_3$ .

The timing data are used by the vehicle library to calculate the front velocity and the rear velocity of a detected vehicle. The software uses the time interval of the two sensors and distance between them to calculate the front velocity  $v_0$ ,

$$v_0 = \frac{d}{t_1 - t_0}$$

where  $d$  is the distance between the two sensors. The rear velocity is calculated in a similar fashion

$$v_1 = \frac{d}{t_3 - t_2}$$

The velocities are used to calculate the average acceleration of the vehicle as it passed under the two laser sensors. The calculation is based on the front velocity,  $v_0$ , and the rear velocity,  $v_1$ , and the first edge for the first sensor,  $t_0$ , and the first edge of the second sensor,  $t_2$ ,

$$a = \frac{v_1 - v_0}{t_2 - t_0}$$

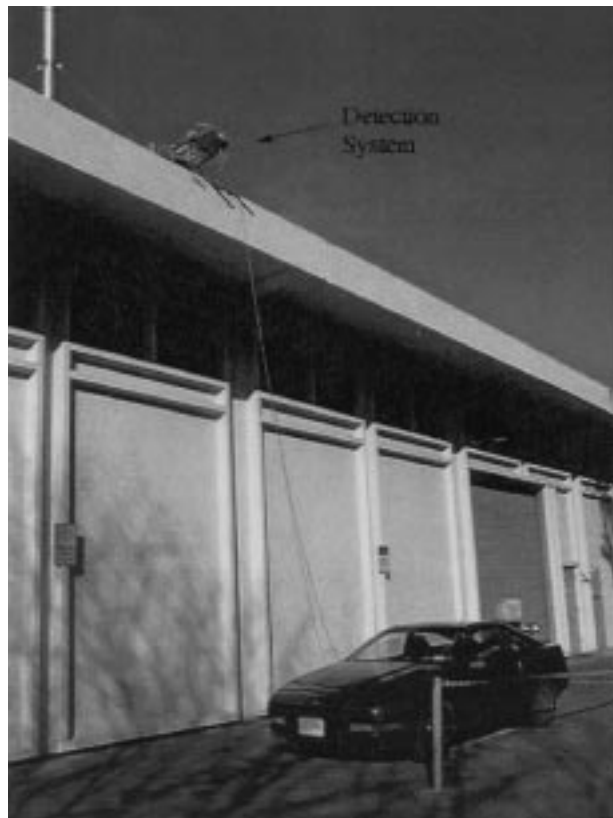


Fig. 18. Bainier Hall testing configuration.

The length of the vehicle is determined from the front velocity, the timing of the first edges and the average acceleration

$$l = v_0(t_2 - t_0) + \frac{1}{2}a(t_2 - t_0)^2$$

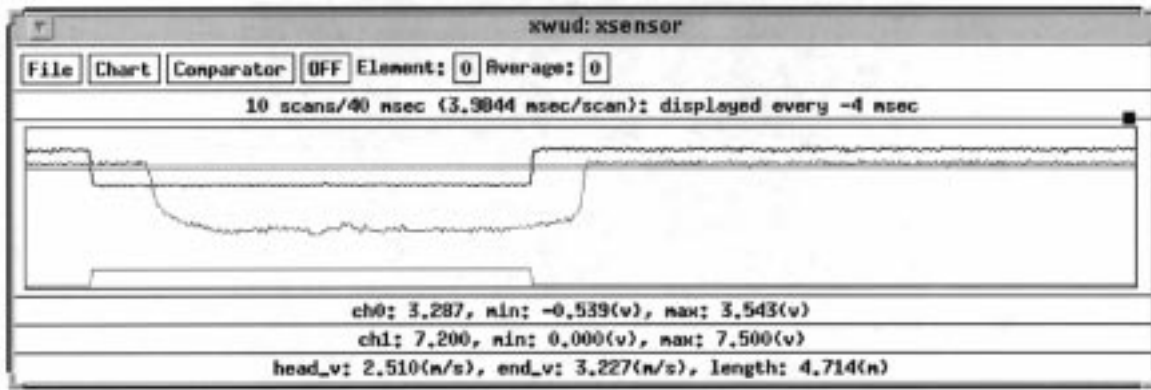


Fig. 19. Bainer Hall testing results.

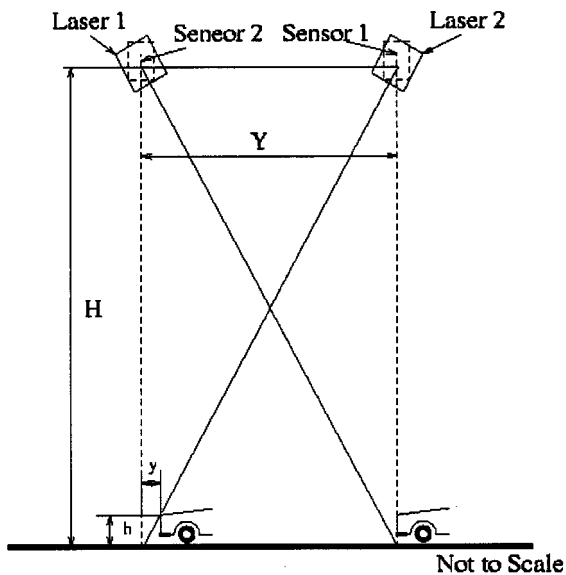


Fig. 20. Schematic showing measurement errors associated with the detector system geometry.



Fig. 21. Detector system shown in place at a highway test site.

The vehicle delineation library groups all of the above calculated parameters into one structure and makes the data available for reading by an application. The group contains the timing information, the front and rear velocities, average acceleration and finally the calculated length of the vehicle.

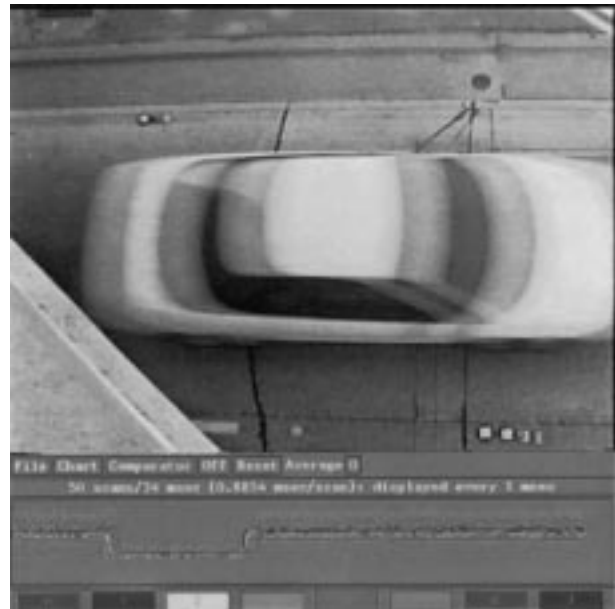


Fig. 22. Outdoor test results showing the laser detector signals. Also shown is a video image of the vehicle that produced the signals. The vehicle image is blurred because of the speed of the vehicle.

## VII. EXPERIMENTAL RESULTS

Outdoor testing of the development system, shown in Fig. 17, was conducted at the Bainer Hall site at UC Davis using a full-size vehicle, as shown in Fig. 18. The results, shown in Fig. 19, were collected primarily to verify the proper operation of the system components. During this testing, a total of eight elements (four elements from each sensor array) was used. From the testing result, we can notice that the vehicle blocks the lasers sequentially. The displayed data show that the speed of the front of the vehicle was around 5.615 mi/h (2.510 m/s), the rear speed was around 7.219 mi/h (3.227 m/s) and the length was around 4.714 m. The rear speed was larger than the front speed because the vehicle was accelerating. The critical height was around 46 cm (18 in), near the desired value. The accuracy of the vehicle length is better than a few centimeters in different tests. The accuracy is directly related to the laser pulse and data acquisition rates. In these tests the laser pulse and data acquisition rates were 2.2 kHz. The accuracy can be improved considerably simply by increasing these rates to 10 kHz, which

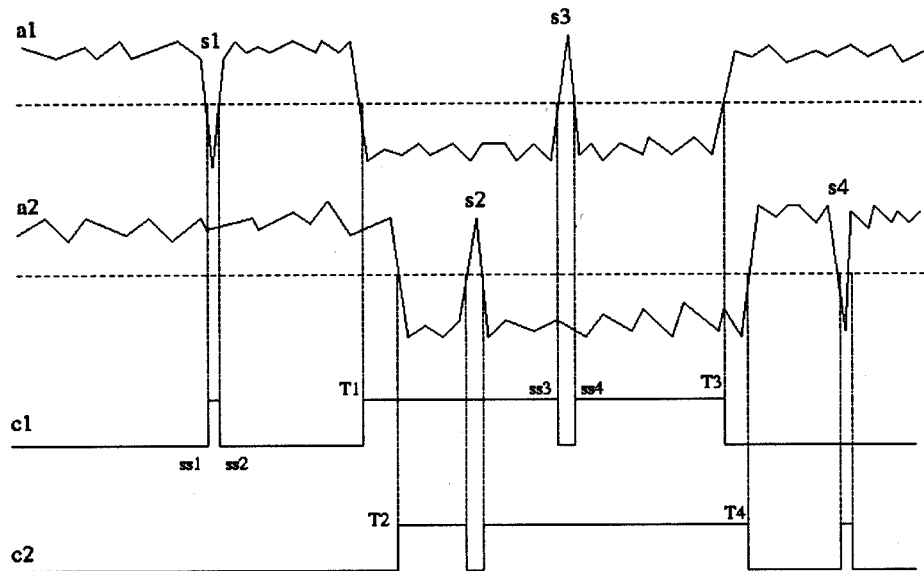


Fig. 23. Schematic showing data spikes and detector state transitions.

is the maximum pulse rate available with the present lasers. The minimum vehicle length uncertainty associated with finite data rates,  $\delta l$ , may be simply estimated as  $\delta l = nv/f$ , where  $v$  is the vehicle speed,  $n$  the number of laser pulses missed (if any) because of any ambiguity in the state transition in the data acquisition system, and  $f$  the data rate (the laser frequency). For the representative values  $n = 1$  to  $3$ ,  $f = 2.2$  kHz, and  $v = 120$  km/h, it is found that  $\delta l = 1.5$  to  $4.5$  cm. For the faster data rate  $f = 10$  kHz, it is found that  $\delta l = 0.33$  to  $1.0$  cm, which is significantly smaller. It is also noted that since multiple detector elements are used, averaging could be employed to reduce the magnitudes of random measurement errors.

We tested the system at Bainer Hall several times in different temperature and weather conditions including day and night, sunshine and fog. The results were consistent. The actual length of the vehicle was around 4.5 m. The difference between the actual length and the measured length is due in part to the geometry of the detection system (and also the laser pulse and data acquisition rates). As can be seen in Figs. 2 and 3, the paths of the two lasers are not parallel to each other. Because of this, the velocity and length measurements have some dependence on the height of the vehicle. This is shown more clearly in Fig. 20, which illustrates the front of a vehicle as it passes below the two laser and sensors comprising a detection system. From this figure, it is clear that the error,  $y$ , associated with the length measurement is related to the effective vehicle height,  $h$ , the detector system height,  $H$ , and the detector spacing,  $Y$ , via the equation  $y = hY/H$ . For the representative values  $Y = 0.305$  m,  $h = 1$  m, and  $H = 6.4$  m, it is found that  $y = 0.048$  m (4.8 cm). While this type of error is fixed for given vehicle and detector geometries, it should be repeatable and scalable between detection sites and therefore should not cause a problem. As long as measurements are consistent between sites, to perform vehicle identification it should be necessary only to measure a representative vehicle length rather than the true length.

Following the successful outdoor tests at the Bainer Hall test site, the laser detector system was tested at a California Department of Transportation highway test site. At this test site, the detector system was mounted on a highway overpass above Interstate Highway 5. An image of the apparatus mounted at this test site is shown in Fig. 21. This image shows the mounting frame as well as some of the electronic circuitry. The lasers and receiving optics are not visible in this view. A video camera was also used at the test site to record images of vehicles passing underneath the detector system—a representative video image of a passing vehicle is shown in Fig. 22. Signals from the detector system, which were produced by this vehicle, are also shown in this figure. It is apparent in Fig. 22 that the signal-to-noise ratio is good and the transitions between states where the laser is blocked and where it is not are relatively sharp, though some improvement can be made in this regard. As a result, new circuitry has been designed which has much faster time response and significantly lower levels of noise—this circuitry will be described in a later publication.

These highway test results were obtained under relatively good weather conditions. It is obviously of interest to determine the response of the detector system under conditions of heavy snow or rain. These types of tests will be performed at a future date, after detector units have been sealed and made useable in wet conditions. It is worth noting, however, that tests at the Bainer Hall site have indicated that the system will work properly with wet pavement, suggesting that rain will not cause significant problems with detector operation.

In real-time detection, there may be some noise in the signal. Some of this noise appears as spikes. Using analog or digital filtering can reduce or eliminate this kind of noise, but such filtering will increase the hardware complexity and can add extra system delays. In our software design, a sequence-based analysis is used to remove the influence of spike noise, as described below.



Assume a pair of laser-sensor systems is used to detect the presence of a vehicle. In Fig. 23,  $a_1$  is the original signal of the first laser-sensor and  $a_2$  is the original signal of the second laser-sensor. This two-detector system is adjusted to detect the same point of a vehicle. The original analog signals are converted to binary signals through comparator windows. The signal  $c_1$  is the binary signal of  $a_1$  and  $c_2$  is the binary signal of  $a_2$ . The spike noises  $s_1$ ,  $s_2$ ,  $s_3$ , and  $s_4$  also appear in the binary signals. It is obvious that vehicle absence signal should be in a logical sequence such as  $c_1$  rising (T1),  $c_2$  rising (T2),  $c_1$  down (T3), and  $c_2$  down (T4). If there is a spike ( $s_1$ ) in  $a_1$  where a vehicle is not in the detection zone, the edge sequence of the binary signal shall be  $c_1$  rising (ss1) followed by  $c_1$  falling (ss2), while  $c_2$  does not change. In this case we view  $s_1$  as noise and ignore it. The same case is shown in  $s_4$ . If the spike occurs while the vehicle is in the detection zone, such as  $s_3$ , the software checks the sequence of the edges. In this case,  $c_1$  rises (T1),  $c_2$  rises (T2),  $c_1$  falls (ss3), and  $c_1$  rises (ss4). When the software determines that  $c_1$  rose twice (T1 and ss4) while  $c_2$  does not fall, it will judge that  $s_3$  is noise because between the two rises of  $c_1$ , it should have  $c_2$  falling. The software will then view  $s_3$  as noise and ignore it. Similar programming allows the  $s_2$  spike to be ignored by the software. The algorithm cuts out most spike noise while not adding any extra system delays. Spike noise that is not cut out produces erroneous data that is easily rejected by the software.

### VIII. CONCLUSIONS

We have introduced an alternate method to the use of VAP. The system we have developed is mounted above the road and, as a result, is relatively easy to install. The system is insensitive to ambient lighting conditions due to its active signal source (the laser). The data gathered by the sensor are computationally easy to process. A series of preliminary indoor tests with model cars and outdoor tests using actual passenger vehicles have been performed to verify our method of speed and length measurement, which can be used to distinguish characteristics of moving vehicles on the highway. We have successfully designed and built the optics and electronics for the system. The prototype system has provided us with useful data that have verified the validity of our design.

### IX. DISCUSSIONS

The above described prototype detection system is a proof-of-concept implementation. In the future we intend to extend the system to include additional detection methods and improvements. In this section some possible improvements are described.

As mentioned previously, each sensor array has 25 elements, however only four are currently used on each sensor. In the future it would be useful to use all 25 elements, or to use an array with additional elements. More elements would provide greater lateral resolution and would allow us to determine the lateral shape of laterally symmetrical objects such as vehicles. We could use the coefficients of a curve fit of this curvature as additional feature vectors that would help delineate vehicles

with the same length from one another. It is also of interest to perform further studies to optimize the geometry of the sensors with a goal of maximizing the system resolution. This may also allow reducing the number of sensors, which could reduce the overall system cost.

The detector could also be modified to determine the differential chromatic reflectance, of vehicles as another delineating feature. This is basically the quantitative ratio of laser light of different frequencies reflected off the same part of the vehicle at the same emitter-detector angle. Because the ratio will vary with the reflective properties of the individual vehicle part, the mode value will represent IR reflectance of the predominant color of the vehicle. This would be incorporated into this detector prototype most easily using the same optics by inserting a 760- and 840-nm laser in the same plane as sensor 1 in Fig. 3 and incorporating a sub-900 nm mirror between the Telescopic Lens and Optical Filter in Fig. 8. The sub-900 reflection would then be split and filtered into 760- and 840-nm components. Because the reflectance off the vehicle is expected to be much higher than off the pavement, CW lasers and a single element photodiode, or a photodiode array with a few elements, could be possibly used, thereby significantly lowering cost.

It is necessary for this detector to determine the precise length of a vehicle in stop-and-go traffic when a nonlinear change in velocity between the front and back bumpers can yield an erroneous vehicle length. By incorporating two of the above configurations used for differential chromatic reflectance in each return optical plane, it is possible to use the peak reflectance sequences as a pattern that can be re-recognized between the detectors in each plane. This will allow the determination of the change in velocity of the vehicle while it is under the detector, which will allow much more precise determination of vehicle lengths at low speeds.

It is also anticipated to modify this system so that it can be used for in-situ vehicle pollutant detection. This might be accomplished by simply changing the frequency of the laser line generator in Fig. 1 so that the pollutant absorbs the laser light. After the vehicle passes the detector, the reflection of the laser off the pavement will be attenuated by the quantity of pollutants emitted. By the time the next vehicle arrives, its turbulent wake will entrain enough surrounding air to allow a fresh pollution measurement. This has advantages over present in-situ vehicle pollutant detectors in that it integrates the entire area behind the vehicle and is not subject to misreading due to turbulent fluid flows, and it is not a horizontally operated detector so it can be used to individually assess multiple lanes.

### REFERENCES

- [1] M. Ostland, K. F. Petty, P. Bickel, J. Jiang, J. Rice, Y. Ritov, and F. Schoenberg, "Simple travel time estimation from single-trap loop detectors," *Intellimotion*, vol. 6, no. 1, pp. 4-11, 1997.
- [2] C. A. MacCarley, "Advanced imaging techniques for traffic surveillance and hazard detection," *Intellimotion*, vol. 6, no. 2, pp. 6-15, 1997.
- [3] J. Malik and S. Russell, "Measuring traffic parameters using video image processing," *Intellimotion*, vol. 6, no. 1, pp. 6-13, 1997.
- [4] J. Palen, "The need for surveillance in intelligent transportation systems," *Intellimotion*, vol. 6, no. 1, pp. 1-10, 1997.
- [5] B. A. Coifman, "Vehicle reidentification and travel time measurement using loop detector speed traps," Ph.D. dissertation, Univ. California, Berkeley, 1998.

- [6] H. H. Cheng, B. D. Shaw, J. Palen, J. E. Larson, X. D. Hu, and V. K. Katwyk, "A real-time laser-based detection system for measurement of delineations of moving vehicles," in *ASME 19th Computers in Engineering Conf.*, Las Vegas, NV, Sept. 12–15, 1999, paper DETC99/CIE-9072.
- [7] R. M. Tyburski, "A review of road sensor technology for monitoring vehicle traffic," *ITE J.*, vol. 59, no. 8, Aug. 1989.
- [8] G. A. Halvorson, "Automated real-time dimension measurement of moving vehicles using infrared laser rangefinders," M.S., Univ. Victoria, 1995.
- [9] R. A. Olson, R. L. Gustavson, R. J. Wangler, and R. E. McConnell II, "Active near-field object sensor and method employing object classification techniques," U.S. patent 5 321 490, 1994.
- [10] R. J. Wangler, R. L. Gustavson, R. E. McConnell II, and K. L. Fowler, "Intelligent vehicle highway system sensor and method," U.S. Patent 5 546 188, 1996.
- [11] —, "Intelligent vehicle highway system sensor and method," U.S. Patent 5 757 472, 1998.
- [12] —, "Intelligent vehicle highway system multi-lane sensor and method," U.S. Patent 5 793 491, AU: PLEASE SUPPLY MONTH AND DAY 1998.
- [13] LynxOS Real-Time Operating System Overview (1999). [Online]. Available: <http://www.lynx.com/products/lynxos.html>
- [14] B. O. Gallmeister, *POSIX.4: Programming for the Real World*. Sebastopol, CA: O'Reilly & Associates, Inc., 1995.
- [15] P. Horowitz and W. Hill, *The Art of Electronics*, 2nd ed. New York: Cambridge Univ. Press, 1989.



**Harry H. Cheng** received the M.S. degree in mathematics and the Ph.D. degree in mechanical engineering from the University of Illinois at Chicago in 1986 and 1989, respectively.

He is an Associate Professor and the Director of the Integration Engineering Laboratory in the Department of Mechanical and Aeronautical Engineering at the University of California, Davis. His current research interests include extending C/C++ for ubiquitous computing and scripting, engineering software design, Web technology and its applications in design and manufacturing, and open-architecture system integration. He had participated in revision of the latest C Standard called C99 through ANSI X3J11 and ISO S22/WG14 C Standard Committees since 1993. Before joining the faculty at UC Davis, he worked as a senior engineer at Research and Development, United Parcel Service, Inc. from 1989 to 1992.

Dr. Cheng received a Research Initiation Award from the National Science Foundation in 1993, the Procter and Gamble Best Paper Award at the 1993 Third National Conference on Applied Mechanisms and Robotics, the Kenneth J. Waldron Award for his work on mechanisms and robotics in 1995. He received an Outstanding Contribution Award from United Parcel Service, Inc. in 1990. He was awarded three University Fellowships from the University of Illinois at Chicago (1986–1987, 1987–1988, 1988–1989). He is an Associate Editor of *ASME Trans. Journal of Computing and Information Science in Engineering*.

**Benjamin D. Shaw** received B.S. and M.S. degrees in mechanical engineering from Colorado State University in 1981 and 1984, respectively, and the Ph.D. degree in mechanical and aerospace engineering from Princeton University, Princeton, NJ, in 1989.

He also was a Post-Doctoral researcher at the University of California, San Diego for the period 1988 to 1989. He was a faculty member in the mechanical engineering department at the University of Connecticut from 1989 to 1991. In 1991 he joined the Mechanical and Aeronautical Engineering Department at the University of California, Davis, as a faculty member, where he is currently an Associate Professor. His research interests include applied mathematics, combustion, microgravity phenomena and transportation.



**Joe Palen** is currently working for the Caltrans New Technology and Research Program. He has managing and/or been a technical consultant for more than 100 projects in various aspects of transportation research, primarily focused on evaluating and improving real time operational efficiency. This experience has caused him to become increasingly concerned how inefficiently real time transportation "state" information is generated and used. He is recognized as a leading authority on advanced detection system R&D in transportation.

Mr. Palen is a Professional Registered Engineer in the State of California.

**Jonathan E. Larson** received the B.S. and M.S. degree in mechanical engineering from the University of California, Davis, in 1996 and 2001, respectively.

Currently, he is a Software Engineer for AKT America Inc., Santa Clara, CA. AKT is a leading supplier of chemical vapor deposition equipment for thin film transistor liquid crystal display manufacturing.



**Xudong Hu** was born in Wenzhou, China, in 1959. He received the B.S. and M.S. degrees in mechanical engineering in the Zhejiang Institute of Science and Technology, China, in 1983 and 1989, respectively.

From 1997 to 2000, he was a visiting scholar in Mechanical and Aeronautical Engineering Department at the University of California, Davis. Since 1995, he has been an Associate Professor of mechanical engineering in the Zhejiang Institute of Science and Technology, China where he is an executive associate director of the Center of Integration

Engineering. His research interests include mechatronics, open-architecture enterprise-level system integration, microcontroller system design, robotics, and modern manufacturing.

**Kirk Van Katwyk** received the B.S. and M.S. degrees in mechanical engineering from the University of California, Davis, in 1995 and 2000, respectively.

He was a Research Assistant for the Integration Engineering Laboratory at UC Davis and wrote engineering analysis software, device drivers for a real-time operating system and data-acquisition software for the laser-based detection system. In 1998, he joined Applied Materials, Inc., Santa Clara, CA, as a Software Engineer for the Robotics group of the Synexis™ Common Platform Products division. He currently develops software for 300-mm automation products and conducts concept and feasibility studies of new control technologies.